

Research Article

Clarithromycin, Midazolam, and Digoxin: Application of PBPK Modeling to Gain New Insights into Drug–Drug Interactions and Co-medication Regimens

Daniel Moj,¹ Nina Hanke,¹ Hannah Britz,¹ Sebastian Frechen,² Tobias Kanacher,² Thomas Wendl,² Walter Emil Haefeli,³ and Thorsten Lehr^{1,4}

Received 24 June 2016; accepted 25 October 2016; published online 7 November 2016

Abstract. Clarithromycin is a substrate and mechanism-based inhibitor of cytochrome P450 (CYP) 3A4 as well as a substrate and competitive inhibitor of P-glycoprotein (P-gp) and organic anion-transporting polypeptides (OATP) 1B1 and 1B3. Administered concomitantly, clarithromycin causes drug–drug interactions (DDI) with the victim drugs midazolam (CYP3A4 substrate) and digoxin (P-gp substrate). The objective of the presented study was to build a physiologically based pharmacokinetic (PBPK) DDI model for clarithromycin, midazolam, and digoxin and to exemplify dosing adjustments under clarithromycin co-treatment. The PBPK model development included an extensive literature search for representative PK studies and for compound characteristics of clarithromycin, midazolam, and digoxin. Published concentration–time profiles were used for model development (training dataset), and published and unpublished individual profiles were used for model evaluation (evaluation dataset). The developed single-compound PBPK models were linked for DDI predictions. The full clarithromycin DDI model successfully predicted the metabolic (midazolam) and transporter (digoxin) DDI, the acceptance criterion ($0.5 \leq AUC_{\text{ratio,predicted}}/AUC_{\text{ratio,observed}} \leq 2$) was met by all predictions. During co-treatment with 250 or 500 mg clarithromycin (bid), the midazolam and digoxin doses should be reduced by 74 to 88% and by 21 to 22%, respectively, to ensure constant midazolam and digoxin exposures (AUC). With these models, we provide highly mechanistic tools to help researchers understand and characterize the DDI potential of new molecular entities and inform the design of DDI studies with potential CYP3A4 and P-gp substrates.

KEY WORDS: clarithromycin; digoxin; dose; drug interaction; midazolam; PBPK.

INTRODUCTION

Pharmacokinetic (PK) drug–drug interactions (DDIs) can cause negative clinical effects, either by decreasing therapeutic efficacy or by enhancing toxic side effects of drugs. DDIs play an important role in reported adverse events (1) and are a major cause of market withdrawal of drugs due to safety reasons (2). To cope with the increasing DDI risks associated with polypharmacy, the European

Medicines Agency (EMA) (3) and the US Food and Drug Administration (FDA) (4) published guidance documents to help researchers understand and characterize the DDI potential of new molecular entities. A prominent feature of these guidances is the recommendation of well-established perpetrator and victim drugs for clinical DDI studies. Perpetrators of metabolic DDIs inhibit or induce, e.g., cytochrome P450 (CYP) enzymes. CYP enzymes are an important source of clinically relevant DDIs, among which CYP3A4 is the most common enzyme for the metabolic clearance of drugs (5,6). Consequently, the inhibition or induction of CYP3A4 is a frequent cause of DDI.

Until 2013, ketoconazole has been the CYP3A inhibitor of choice in clinical DDI studies (7). Due to the risk of serious hepatic toxicity, the EMA and the FDA advised against the further use of ketoconazole in clinical DDI studies (8). Clarithromycin has been proposed as a useful clinical alternative (9).

Clarithromycin is a widely prescribed antibiotic (10) that is mainly metabolized via CYP3A4 (11). It forms a non-covalent metabolic-intermediate complex with CYP3A4 (12) leading to a

Electronic supplementary material The online version of this article (doi:10.1208/s12248-016-0009-9) contains supplementary material, which is available to authorized users.

¹Department of Pharmacy, Clinical Pharmacy, Saarland University, Campus C2 2, 66123, Saarbruecken, Germany.

²Computational Systems Biology, Bayer Technology Services GmbH, Leverkusen, Germany.

³Department of Clinical Pharmacology and Pharmacoepidemiology, University of Heidelberg, Heidelberg, Germany.

⁴To whom correspondence should be addressed. (e-mail: Thorsten.Lehr@mx.uni-saarland.de)

mechanism-based inhibition (MBI). This MBI is characterized by a non-linear, dose-dependent and irreversible degradation of CYP3A4. Thus, the MBI by clarithromycin leads to a mechanism-based auto-inhibition of metabolism and results in a non-linear increase of clarithromycin exposure after ascending doses of clarithromycin (13). Clarithromycin is also a substrate (14) and competitive inhibitor of P-glycoprotein (P-gp) (15) as well as a substrate (16,17) and competitive inhibitor of human organic anion-transporting polypeptides (OATP) 1B1 and 1B3 (18).

One of the recommended and most suitable victim drugs to investigate CYP3A4-mediated DDIs is midazolam. Midazolam is a short-acting, widely used sedative approved as premedication before medical interventions that is almost exclusively metabolized by CYP3A4 (19).

Digoxin is a prominent victim drug to investigate P-gp-mediated DDIs, as its disposition is mainly governed by P-gp. Any metabolism via phase I or II enzymes seems to be negligible. The primary route of digoxin elimination (~75%) is renal excretion via glomerular filtration and active tubular secretion (mainly via P-gp) of unchanged drug (20,21). Digoxin binds to and inhibits several subunits of the (Na⁺,K⁺-)ATPase, in particular the subunit alpha 2, which leads to the desired positive inotropic effects of digoxin in the heart (22).

OBJECTIVE

The aims of this work were as follows:

1. To develop fully mechanistic physiologically based pharmacokinetic (PBPK) models for the single compounds clarithromycin, midazolam, and digoxin
2. To couple the clarithromycin and midazolam PBPK models to predict the metabolic DDI (via CYP3A4) of these two drugs
3. To couple the clarithromycin and digoxin PBPK models to predict the transporter-based DDI (via P-gp) of these two drugs

Exemplarily, it is shown how dosing recommendations for midazolam and digoxin during co-administration with various doses of clarithromycin can be derived.

METHODS

PBPK Model Development

The PBPK model development consisted of (i) an extensive literature search for representative PK studies and (ii) for compound characteristics (physicochemical and ADME) of clarithromycin, midazolam, and digoxin. For the model development, the available, published, and unpublished individual PK data were divided into a “training” dataset for model development and an “evaluation” dataset for model qualification. The training dataset was used to optimize model parameter values to find the best overlap between observed and simulated concentration-time profiles. First, intravenous concentration-time profiles were used to determine clearance and distribution parameters. Second, oral concentration-time profiles were used to determine absorption and dissolution parameters, keeping the formerly optimized parameters fixed. Model qualification with the

evaluation dataset was carried out using visual predictive checks. The final single-compound models were then coupled to predict the pharmacokinetic effects of clarithromycin on midazolam and digoxin. The PBPK models for clarithromycin, midazolam, and digoxin were developed independently of each other. This also includes the parameterization of the CYP3A4 MBI, which has been achieved with multiple-dose studies of clarithromycin only. The parameters for the inhibition of P-gp have been taken from *in vitro* experiments without optimization. DDI PK studies were used to qualify the DDI prediction performance of the coupled clarithromycin–midazolam and clarithromycin–digoxin models. Forty-four concentration-time profiles were used in the model development process (Table I).

PBPK modeling software PK-Sim® 5.3.2 (Bayer Technology Services, Leverkusen, Germany) and MoBi 3.3.2 (Bayer Technology Services, Leverkusen, Germany) were used. Statistical analysis of the results and graphics were compiled with Matlab 2015a. Data was digitized using GetData Graph Digitizer 2.25.

PBPK Model Structure

The PBPK models of clarithromycin, midazolam, and digoxin are based on a generic 22-organ PBPK model, including the arterial and venous blood pools and the portal vein. Each organ is further divided into sub-compartments, characterizing the blood plasma, the red blood cells (RBC), the interstitial space, and the intracellular space. The mass transfer between compartments is based on a generic distribution model (passive processes). Herein, substance-specific parameters (*e.g.* lipophilicity) are used to determine permeabilities across membranes and partition coefficients between compartments. Active processes (binding, metabolism, and transport) are additionally implemented, depending on the PK behavior of the substance.

For clarithromycin, implemented active processes are metabolism via CYP3A4 and transport via OATP 1B3. An unspecific renal clearance of clarithromycin was assumed. As P-gp substrate, the intestinal absorption of clarithromycin is reduced by intestinal P-gp. The impact of this efflux transport of clarithromycin from intestinal mucosa to intestinal lumen was implemented by reducing the net transcellular intestinal permeability of clarithromycin (55). The midazolam model assumes metabolism by CYP3A4 with negligible renal clearance. The digoxin model incorporates active efflux transport via P-gp with a renal clearance of digoxin consisting of glomerular filtration and tubular secretion by P-gp.

The PBPK modeling software calculates the organ-specific protein expression relative to the expression in the organ with the highest concentration of the respective protein (reference concentration). The reference concentration corresponds to an expression level of 100%. Hence, organ-specific transporter protein concentrations of P-gp and OATP 1B3 used in simulations were calculated based on Eq. 1,

$$C_{T,organ} = T_{REF} \times \text{EXPR}_{organ} \quad (1)$$

where $C_{T,organ}$ denotes the molar transporter concentration in the specific organ, T_{REF} is the transporter reference

Table I. Clinical Study Data of Clarithromycin, Midazolam, and Digoxin in Healthy Volunteers

Substrate	Route of administration	Dose [mg]	Number	Age range (mean) [years]	Weight range (mean) [kg]	Height range (mean) [cm]	BMI range (mean) [kg/m ²]	Ref.
Clarithromycin	iv (inf, 0.5 h, SD)	0.1	30	18–55	–	–	18–30	(23)
	iv (inf, 0.5 h, SD)	250	22	18–40 (29)	57.7–87.7 (71.5)	164–188 (175)	–	(24)
	po (tab, SD)	100–1200	36	19–36 (25.3)	55.9–96.6 (71.4)	158–191 (175)	–	(13)
	po (tab, MD)	250	17	18–40 (29)	57.7–87.7 (70.8)	164–188 (174.9)	–	(25)
	po (tab, MD)	250	12	21–39 (28)	68–98 (80)	–	22–28 (24)	(26) ^b
	po (tab, MD)	250, 500	12	24–38 (26.5)	65–88 (79.5)	168–197 (182)	–	(27)
	po (tab, MD)	500	17	20–39 (31)	63.9–86.8 (72.2)	160–183 (174.1)	–	(25)
	po (sol, MD)	500	12	19–41 (28)	45.1–86.1 (66.5)	150–186 (168.4)	–	(28)
Midazolam	iv (inf, 0.5 h, SD)	0.05/kg	16	(34)	(78)	–	–	(29)
	iv (bolus, SD)	0.13/kg	5	28–49	70–80	–	–	(30)
	iv (bolus, SD)	1.0	12	18–50	–	–	18–30	(31)
	iv (bolus, SD)	1.0	19	(22.9)	(68.1)	(174)	–	(32)
	iv (bolus, SD)	5.0	6	21–22	66.3–77.0	–	–	(33)
	iv (bolus, SD)	5.0	12	20–45 (29) ^a	–	–	20–26 (23) ^a	(34)
	iv (bolus, SD)	11.42	6	22–27	55–77	–	–	(35)
	po (sol, SD)	2.0	12	18–50	–	–	18–30	(31)
	po (sol, SD)	3.0	11	(31.2)	–	–	(23)	(36)
	po (tab, SD)	4.0	16	(34)	(78)	–	–	(29)
	po (sol, SD)	5.0	24	–	–	–	–	(37)
	po (tab, SD)	7.5, 15, 30	12	24–52	54.9–92.5	–	–	(38)
	po (tab, SD)	10.0	6	21–22	66.3–77.0	–	–	(33)
	po (tab, SD)	15.0	12	24–53	54–93	–	–	(39)
	Digoxin	po (tab, SD)	10.0, 20.0	6	22–27	55–77	–	–
iv (inf, 0.08 h, SD)		0.01/kg	12	21–39 (28)	68–98 (80)	–	22–28 (24)	(26)
iv (bolus, SD)		1.0	12	–	–	–	–	(40)
iv (bolus, SD)		0.5	6	–	66–96	–	–	(41)
iv (bolus, SD)		0.015/kg	6	22–29 (24)	–	–	–	(42)
iv (inf, 0.08 h, SD)		0.5	12	(28)	(74)	–	(23)	(43)
iv (inf, 0.5 h, SD)		1.0	8	(29)	(84)	–	–	(44)
iv (inf, 1 h, SD)		0.5	9	(27.9)	(66.6)	(169.7)	–	(45)
iv (inf, 1 h, SD)		0.75	8	–	–	–	–	(20)
iv (inf, 1 h, SD)		0.5, 1.0, 1.5	9	23–37 (31.3)	69–90 (77.7)	–	–	(46)
iv (inf, 1, 3 h, SD)		0.5	6	–	66–96	–	–	(41)
po (tab, SD)		0.5	12	22–35 (26)	–	–	19–28 (22)	(47)
po (tab, SD)		0.25	18	(30)	(77.5)	–	–	(48)
po (na, SD)		0.25	16	20–43 (39) ^a	(72.5) ^a	(174) ^a	(24) ^a	(49)
po (tab, SD)		0.75	12	21–39 (28)	68–98 (80)	–	22–28 (24)	(26)
po (tab, SD)		1.0	8	(29)	(84)	–	–	(44)
po (tab, SD)		1.0	10	19–27 (24) ^a	61–92 (73) ^a	–	–	(50)
po (sol, SD)		0.5	6	–	66–96	–	–	(41)
po (tab, MD)		0.5, 0.25 ^c	8	(32.4)	(74.8)	(178.5)	–	(51)
po (na, MD)		0.125	12	18–55 (37.8)	70–95 (87.8)	(179)	23–30 (27)	(52)
po (tab, MD)	0.25	20	23–49	(74.8)	(171)	(25)	(53)	
po (na, MD)	0.25	22	18–45	(50)	–	–	(54)	

inf infusion, *iv* intravenous, *MD* multiple doses, *na* information not available, *po* per oral, *SD* single dose, *sol* solution, *tab* tablet,

^a Median given

^b Individual concentration-time profiles are unpublished in-house data

^c 0.5 mg bid for 3 days followed by 0.25 mg bid for 2 weeks

concentration, and $EXPR_{organ}$ denotes the transporter expression relative to the organ with the highest concentration (56–58).

In our models, CYP3A4 is expressed in the liver and the intestinal mucosa. The CYP3A4 reference concentration used in the simulations was set to 3.47 $\mu\text{mol/L}$ (59) in the liver. OATP 1B3 is expressed in, *e.g.*, the bone, liver, lung, muscle, and intestine, with the highest OATP 1B3 expression (276

nmol/L (60)) in the intestinal mucosa according to published expression databases (56,57). P-gp was expressed in, *e.g.*, the brain, kidney, liver, and intestine, with the highest expression in the kidney (61) (101 nmol/L (62)). ATPase (subunit alpha 2), as digoxin binding partner, is implemented, *e.g.*, in the brain, heart, and muscle with the highest expression in the brain (57,58), with a fitted reference concentration of 99.5 $\mu\text{mol/L}$.

MBI of CYP3A4 Metabolism

The metabolic clearance (CL_{met}) of clarithromycin and midazolam via CYP3A4 was incorporated using Eq. 2,

$$CL_{met} = V_{max} \times C_t / (K_{M,CYP3A4} + C_t) \text{ with } V_{max} = k_{cat,CYP3A4} \times E_t \quad (2)$$

where C_t denotes the unbound concentration of clarithromycin or midazolam in the respective intracellular organ compartment and $K_{M,CYP3A4}$ denotes the Michaelis-Menten constant of CYP3A4 for the respective substrate. The parameter $k_{cat,CYP3A4}$ is the turnover number and E_t is the amount of CYP3A4 at time point t available for metabolizing processes.

The MBI of CYP3A4 by clarithromycin was implemented and the organ-specific *de novo* synthesis rates were described by Eq. 3,

$$R_0 = E_0 \times k_{deg} \quad (3)$$

where R_0 is the *de novo* protein synthesis rate of CYP3A4, E_0 is the enzyme amount at baseline at time point 0, and k_{deg} denotes the 1st-order degradation rate constant of CYP3A4.

The rate of change of CYP3A4 amount due to the inactivation via clarithromycin in the intracellular compartments was described by Eq. 4,

$$dE_t / dt = R_0 - k_{deg} \times E_t - (k_{inact} \times CLR_t / (K_I + CLR_t)) \times E_t \quad (4)$$

where the maximum rate of enzyme inactivation (k_{inact}) and the concentration required for half-maximal enzyme inactivation (K_I) of clarithromycin are used to describe the enzyme inactivation due to the intracellular, unbound clarithromycin concentration at time point t (CLR_t). Value selection for k_{inact} and K_I (Table II) was based on the descriptive performance of the auto-inhibition in multiple-dose studies of clarithromycin.

Competitive Inhibition of P-gp Transport

The P-gp efflux transport of digoxin (J_{efflux}) was described by Eq. 5,

$$J_{efflux} = J_{max} \times DIG_t / (K_{M,Pgp} + DIG_t) \text{ with } J_{max} = k_{cat,Pgp} \times P_t \quad (5)$$

where DIG_t denotes the unbound concentration of digoxin in the respective intracellular organ compartment and $K_{M,Pgp}$ denotes the Michaelis-Menten constant of P-gp for digoxin. The parameter $k_{cat,Pgp}$ is the turnover number and P_t is the amount of P-gp at time point t available for transporting processes.

The competitive inhibition of P-gp-mediated digoxin transport by clarithromycin was implemented using Eq. 6,

$$K_{M,Pgp,app} = K_{M,Pgp} \times (1 + I / K_i) \quad (6)$$

where $K_{M,Pgp}$ denotes the digoxin Michaelis-Menten constant in the absence of clarithromycin, I is the unbound clarithromycin concentration, and K_i denotes the dissociation constant of the clarithromycin-transporter complex. Using the assumptions of Cheng and Prusoff (88), a P-gp K_i value for clarithromycin of 3.78 $\mu\text{mol/L}$ was used in the simulations, based on a published IC_{50} of 4.1 $\mu\text{mol/L}$ (15).

Drug-Drug Interaction

The AUC_{ratio} ($AUC_{inhibition}/AUC_{normal}$) between the victim drug AUC with clarithromycin co-treatment ($AUC_{inhibition}$) and without clarithromycin co-treatment (AUC_{normal}) was determined. The AUC_{ratio} derived from the DDI model prediction was compared to AUC_{ratio} literature values observed in clinical DDI studies. A ratio of $0.5 \leq AUC_{ratio,predicted}/AUC_{ratio,observed} \leq 2$ was used as the acceptance criterion for a successful DDI prediction.

Virtual population characteristics

Interstudy variabilities of the investigated DDIs were assessed using 10 virtual populations with the same number of study individuals as described in the respective study. In virtual populations, CYP3A4 was log-normally distributed with a geometric mean reference concentration of 3.47 $\mu\text{mol/L}$ and a geometric standard deviation (GSD) of 1.6, based on a coefficient of variation of 53% (89). The standard CYP3A4 half-life in liver and intestinal mucosa was set to 36 and 23 h, respectively (90). In virtual populations, the CYP3A4 half-life was uniformly distributed within 10–140 h in the liver and 12–33 h in the intestine (91). P-gp was normally distributed with a mean reference concentration of 101 nmol/L and a standard deviation (SD) of 40% of the mean (92).

Dosing Recommendations of Midazolam and Digoxin for Clinical Practice

Dosing recommendations for midazolam and digoxin under bid (twice a day) clarithromycin co-treatment were determined as percentage of the midazolam and digoxin dose without co-medication. In the scenario of clarithromycin co-administration, doses of midazolam and digoxin were reduced until the $AUC_{inhibition}$ equaled the AUC_{normal} . For the DDI studies, mean individuals were created (mean of the study age, weight, height, and BMI) to calculate the adapted doses during clarithromycin administration of 25, 50, 100, 200, 300, 400, 500, 600, 700, 800, 900, and 1000 mg bid. For the clinically most relevant clarithromycin doses of 250 and 500 mg, virtual population simulations were performed using the adapted doses of midazolam and digoxin.

Table II. Physicochemical and Pharmacokinetic Parameter Values Used in Simulations

Parameter	Units	Clarithromycin in simulations	Clarithromycin literature	Digoxin in simulations	Digoxin literature	Midazolam in simulations	Midazolam literature	Description
MW	g/mol	747.95	747.95	780.93	780.93	325.77	325.77	Molecular weight
f_u		0.48 ^a	0.28-0.58 (63)	0.70	0.70 (64)	0.025 ^a	0.024-0.08 (65,66)	Fraction unbound
logP		2.3 ^a	2.3-3.24 (23,67)	1.67	1.67 (68)	2.98 ^a	2.7-4.33 (69,70)	Lipophilicity
B:P		1.23	1.23 (PK-SIM) ^b	0.94	0.94 (PK-SIM) ^b	0.61 ^a	0.53-0.7 (35,71)	Blood-to-plasma concentration ratio
pKa		8.99 ^a	8.76-8.99 (72,73)	13.5	13.5 (74)	6.15	6.15 (75)	Acid dissociation constant
Solubility [pH]	g/L	12.17 [2.4]	12.17 [2.4] (76)	17.0	17.0 (77)	0.024 [7]	0.024 [7] (78)	Solubility
P_{plsb}	$\mu\text{m/s}$	0.40 ^c	0.55 (PK-SIM) ^b	0.99	0.99 (PK-SIM) ^b	8.24	8.24 (PK-SIM) ^b	Plasma-blood permeability
P_{bcpls}	$\mu\text{m/s}$	0.03 ^c	0.55 (PK-SIM) ^b	0.99	0.99 (PK-SIM) ^b	8.24	8.24 (PK-SIM) ^b	Blood-plasma permeability
P_{intest}	nm/s	1.12 ^d	3.3 \pm 0.9 (55)	4.42 ^c	16 (79)	26.2 ^c	369 (80)	Intestinal permeability
CYP3A4 K_M	$\mu\text{m ol/}$ L	50.0 ^e	48.7 \pm 17.7 (11)	-	-	2.7	2.7 (81)	Michaelis-Menten constant
CYP3A4 k_{cat}	1/min	11.40 ^c	1.9 \pm 0.7 (11)	-	-	13.1 ^c	1.96 \pm 0.08 (81)	CYP3A4 turnover number
OATP K_M	$\mu\text{m ol/}$ L	50.0 ^e	58.0 \pm 47.9 (16) ^f	-	-	-	-	Michaelis-Menten constant
OATP k_{cat}	1/min	0.15 ^c	8.1 (16) ^g	-	-	-	-	OATP turnover number
P-gp K_M	$\mu\text{m ol/}$ L	-	-	58.2	58.2 (82)	-	-	Michaelis-Menten constant
P-gp k_{cat}	1/min	-	-	173.8 ^c	288.8 (82) ^h	-	-	P-gp turnover number
ATPIA2 k_{off}	1/min	-	-	21.8 ^c	NA	-	-	Dissociation rate constant
ATPIA2 K_d	nmol/L	-	-	25.6	25.6 (83)	-	-	Dissociation constant
CL _R	L/h	7.9 ^a	6.7-12.8 (63)	1	1	1	1	Renal clearance
CYP3A4 K_I	$\mu\text{m ol/}$ L	41.4 ^a	2.25-41.4 (84,85)	-	-	-	-	Inhibition constant
CYP3A4 k_{inact}	h^{-1}	3.3 ^a	2.4-13.8 (86,84)	-	-	-	-	Inactivation rate constant
$D_{T,50}$	min	5.0	c	15.0	c	2	c	Dissolution time (50% dissolved)
Shape factor		2.9	c	0.20	c	0.69	c	Dissolution shape parameter

NA not available

^a Optimized within range of minimum and maximum literature values

^b Calculated internally within PK-Sim

^c Optimized without literature-based value range

^d Optimized within range of mean $\pm 3 \times \text{SD}$

^e Optimized within range of mean $\pm 1 \times \text{SD}$

^f Taken from rat hepatic uptake assessment

^g Assuming 117 million cells per g of rat liver (87)

^h Assuming 275 fmol/cm² of P-gp of mucosal lining (62)

ⁱ For digoxin CL_R consists of GFR and additional renal secretion via P-gp

^j For midazolam CL_R is negligible

Parameter Sensitivity Analysis

Parameter sensitivity analyses have been performed to assess the impact of critical model parameters on the predicted AUC_{ratios} for the co-treatment regimens showing the highest observed AUC_{ratios} . Co-treatment regimens were (i) 500 mg oral clarithromycin at steady state (bid) with a single oral dose of 4 mg midazolam and (ii) 250 mg oral clarithromycin at steady state (bid) with a single oral dose of 0.75 mg digoxin. Assessed parameters were: clarithromycin blood cell permeabilities (one permeability for each direction), CYP3A4 K_I , CYP3A4 k_{inact} , midazolam CYP3A4 k_{cat} , CYP3A4 half-lives in the liver and intestine, digoxin P-gp k_{cat} , digoxin P-gp K_i , and digoxin ATPase k_{off} . All parameters were varied individually over a wide range of values (via multiplication by factors between 0.1 and 10.0) and the change in AUC_{ratio} was documented. If a 10% change of a single parameter leads to a >1% change in AUC_{ratio} , the model is considered sensitive to this parameter.

RESULTS

PBPK models of clarithromycin, midazolam, and digoxin have been successfully developed using the given parameters in Table II. Best simulation results for all compounds were obtained using tissue-to-plasma partition coefficients calculated by the method of Rodgers and Rowland (93,94).

For clarithromycin, it was not possible to adequately describe the concentration-time profile after intravenous administration using standard input parameters (e.g., $\log P$)

and calculation methods (e.g., partition coefficients). Simulated concentration-time profiles over-predicted C_{max} and under-predicted the observed data for time $> T_{max}$. According to literature, clarithromycin accumulates in mononuclear (MN) and polymorphonuclear (PMN) leukocytes, probably via active transport (95). This process was implemented, and it improved the model significantly. Due to limited knowledge on this transport (unknown transporter, unknown V_{max} , and K_M value), an adjustment of the clarithromycin permeability between plasma and RBC compartments was applied. The clarithromycin permeability optimization ($P_{plasma \rightarrow RBC}$, $P_{RBC \rightarrow plasma}$) led to an asymmetric permeability ratio $P_{plasma \rightarrow RBC}/P_{RBC \rightarrow plasma}$ of 13, indicating that clarithromycin can more easily enter than exit the RBC compartments. Using the optimized permeability values, the clarithromycin model successfully described the training dataset's concentration-time profiles after different doses of intravenous (supplementary Fig. 1) and oral clarithromycin application (Fig. 1). The prediction of the evaluation dataset's individual concentration-time profiles was successful for multiple dosing with 250 and 500 mg clarithromycin (Fig. 2) and reasonably well for single rising doses of 100–1200 mg (supplementary Fig. 2). The MBI of CYP3A4 by clarithromycin was successfully implemented. The reported loss of CYP3A4 activity in the liver and intestine (96) during treatment with 500 mg clarithromycin could be accurately simulated (supplementary Fig. 3). Our model predicts a duodenal intracellular mucosa clarithromycin concentration, after oral treatment, which is about 20 times higher than the concentration reached in the intracellular liver compartment

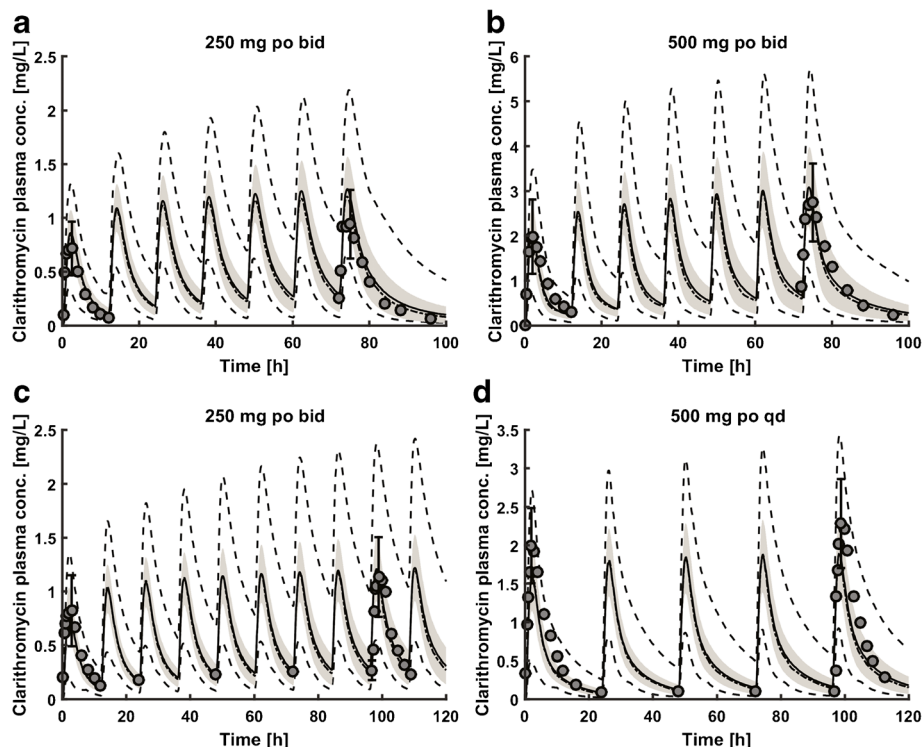


Fig. 1. Predicted concentration-time profiles of clarithromycin after multiple doses of clarithromycin (a, b: ref. (25), c, d: ref. (27)) in comparison with the observed mean data (\pm standard deviation (SD)). Solid line, predicted mean; dashed-dotted line, predicted median; gray shaded area, predicted SD; dashed line, predicted minimum/maximum; gray circles observed mean data (\pm SD)

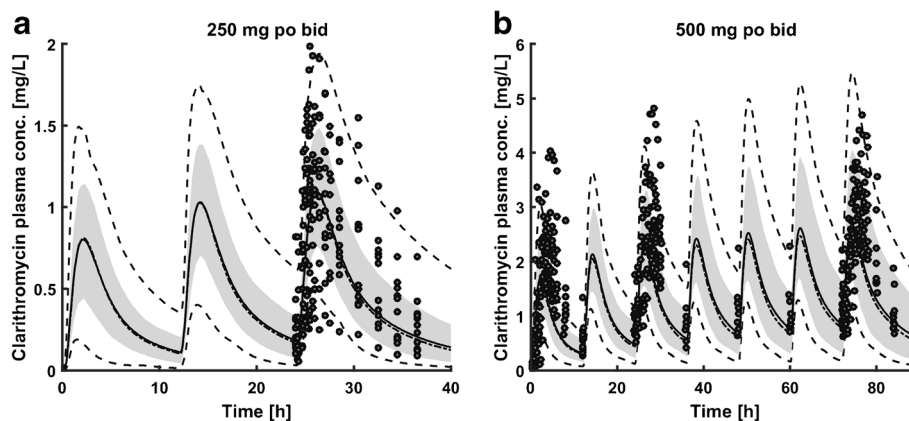


Fig. 2. Predicted concentration-time profiles of clarithromycin after multiple doses of clarithromycin (**a**: ref. (26), **b**: ref. (28)) in comparison with the observed individual data. *Solid line*, predicted mean; *dashed-dotted line*, predicted median; *gray shaded area*, predicted 5th–95th percentile; *dashed line*, predicted minimum/maximum; *gray circles*, observed individual data

($C_{\max, \text{intestine}}$, 621 mg/L; $C_{\max, \text{liver}}$, 31 mg/L). The maximum loss of intestinal CYP3A4 activity was about 80% whereas the hepatic loss was about 55% during simulated treatment with 500 mg clarithromycin bid.

The developed midazolam model appropriately described the training dataset (supplementary Figs. 4 and 5) and predicted the evaluation dataset's concentration-time profiles (Fig. 3, supplementary Figs. 4 and 5), of both, intravenously and orally administered midazolam.

The digoxin model also adequately described the training dataset (supplementary Figs. 6–8) and predicted the evaluation dataset's concentration-time profiles (Fig. 4, supplementary Figs. 6–8) for intravenous and oral administration.

The clarithromycin–midazolam model accurately predicted the clinically observed DDI after oral clarithromycin pretreatment and intravenously or orally administered midazolam (Fig. 5). Hence, the MBI parameter values (k_{inact} , K_I) of the clarithromycin model could be successfully used to predict the clarithromycin–midazolam DDI without further adjustments to these parameters. The clarithromycin–digoxin model adequately predicted the clinically observed DDI after

oral clarithromycin pretreatment and intravenously or orally administered digoxin (supplementary Fig. 9, Fig. 6). The predicted mean $\text{AUC}_{\text{ratios}}$ of the clarithromycin–midazolam DDI, intravenous and oral, were comparable to the observed mean $\text{AUC}_{\text{ratios}}$. Dividing predicted by observed $\text{AUC}_{\text{ratios}}$ gives ratios of 0.8 (minimum) to 1.0 (maximum) (Table III). The predicted mean $\text{AUC}_{\text{ratios}}$ of the intravenous clarithromycin–digoxin DDI were also comparable to the observed mean $\text{AUC}_{\text{ratios}}$. Dividing predicted by observed $\text{AUC}_{\text{ratios}}$ of the intravenous clarithromycin–digoxin DDI gives values of 0.9 (minimum) to 1.0 (maximum). The predicted mean $\text{AUC}_{\text{ratios}}$ of the oral clarithromycin–digoxin DDI were over-predicted by a factor of 2.0. The predicted SDs of all $\text{AUC}_{\text{ratios}}$ (midazolam and digoxin DDI) were close to the observed SDs except for the SD of the clarithromycin–digoxin DDI after intravenous application, which was under-predicted ($\text{SD}_{\text{pred}} = 0.01$ vs. $\text{SD}_{\text{obs}} = 2.22$).

To assess the impact of the parameters used to model the DDI processes, a sensitivity analysis was conducted which showed that 10% changes in CYP3A4 k_{inact} , CYP3A4 K_I , liver CYP3A4 half-life, digoxin P-gp k_{cat} , and midazolam CYP3A4 k_{cat} (5 out of 10 tested parameters) lead to 13, 11,

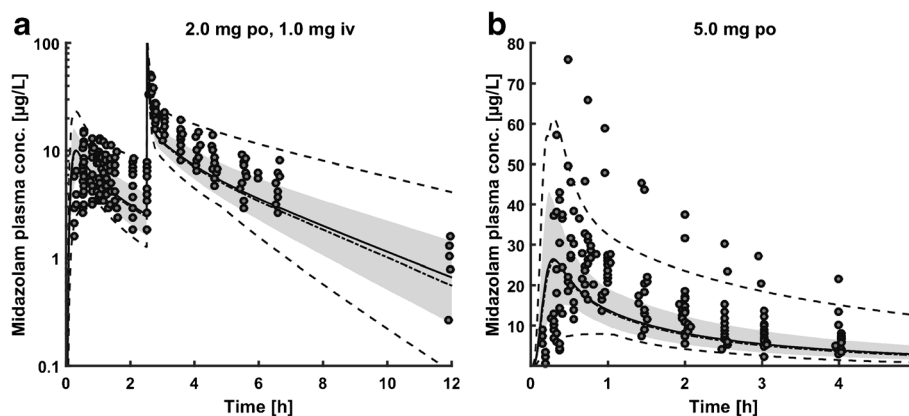


Fig. 3. Predicted concentration-time profiles of midazolam after intravenous and oral doses of midazolam (**a**: ref. (31), **b**: ref. (37)) in comparison with the observed individual data. *Solid line*, predicted mean; *dashed-dotted line*, predicted median; *gray shaded area*, predicted 5th–95th percentile; *dashed line*, predicted minimum/maximum; *gray circles*, observed individual data

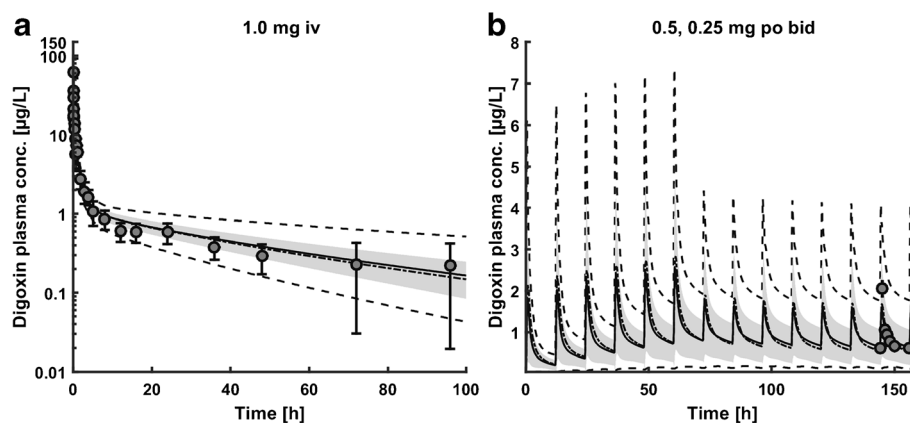


Fig. 4. Predicted concentration-time profiles of digoxin after intravenous and oral doses of digoxin (a: ref. (40), b: ref. (51)) in comparison with the observed mean data (\pm standard deviation (SD)). Solid line, predicted mean; dashed-dotted line, predicted median; gray shaded area, predicted SD; dashed line, predicted minimum/maximum; gray circles, observed mean data (\pm SD)

11, 9, and 5% changes in AUC_{ratios} , respectively (supplementary Fig. 10). The other half of the assessed parameters had no crucial impact on the predicted AUC_{ratios} .

Dosing recommendations for midazolam and digoxin under clarithromycin co-medication were calculated using mean study individuals. An overview of the recommended oral midazolam and digoxin doses with the corresponding oral clarithromycin doses from 25 to 1000 mg bid at steady state is presented in Fig. 7. At clarithromycin steady state with orally administered 500 mg bid, the intravenous midazolam dose had to be reduced by 62% to achieve a similar midazolam exposure as without co-treatment. At clarithromycin steady state with orally administered 250 or 500 mg bid, the oral midazolam doses had to be reduced by 74 and 88%, respectively. During clarithromycin treatment with orally administered 250 or 500 mg bid, the oral digoxin doses had to be reduced by 21 or 22%, to prevent elevated digoxin concentrations.

The identified adjusted midazolam and digoxin doses for co-medication with the clinically most relevant clarithromycin doses of 250 and 500 mg bid were applied in virtual populations (supplementary Table 1). In both DDI scenarios, the number of virtual individuals who experience a relevant increase in the AUC of the victim drug is significantly reduced when applying the adjusted doses. In other words, DDIs take place in all virtual individuals, but the AUCs of the victim drugs stay approximately the same. In the clarithromycin–midazolam DDI, the decline in the number of experienced DDIs is much higher than in the clarithromycin–digoxin DDI using the calculated dose adaptation.

DISCUSSION

For the first time, a whole-body PBPK model of clarithromycin has been developed. The model was able to predict a metabolic and a transporter DDI with the victim drugs midazolam and digoxin.

Apart from our presented whole-body PBPK model, two semi-physiological models of clarithromycin and a commentary on a clarithromycin PBPK model have been published to

date (9,85,97). For the semi-physiological models, empirically accentuated approaches were used, focusing exclusively on the prediction of the impact of clarithromycin on CYP3A4, which was reasonably well predicted. However, the MBIs used in these publications were either available in the liver only or not active at clarithromycin doses \leq 100 mg. Furthermore, these models are not developed for prediction of intravenous application of clarithromycin. In the case of the commentary, no model development was presented, the model structure remains unclear (full or minimal PBPK), and the parameterization was not published.

Our clarithromycin model overcomes these limitations and was built in a more comprehensive and mechanistic approach. The MBI is available in all tissues with CYP3A4 expression and active at all clarithromycin doses after intravenous and oral application. Furthermore, the DDI is not only limited to the level of CYP3A4 but also describes clarithromycin DDIs via P-gp. All three PBPK models (clarithromycin, midazolam, and digoxin) were developed and evaluated independently of each other. Hence, the prediction of the DDIs of clarithromycin with midazolam and digoxin were done without any adaptation of the parameters used in the implemented processes mediating the DDIs. The presented mechanistic models can easily be (i) coupled to other victim or perpetrator models or (ii) expanded by addition of further DDI processes (e.g., OATP inhibition). This comprehensive whole-body PBPK approach was used in the conviction that mechanistic models are better suited for the scaling to special populations like geriatric, pediatric, or diseased populations.

The MBI of CYP3A4 is crucial to understand the non-linear pharmacokinetics of clarithromycin (12). Our model adequately predicts the observed loss of duodenal and hepatic CYP3A4 activity due to the MBI (96). Although CYP3A activity encompasses CYP3A4 and CYP3A5, whose substrate specificities cannot be distinguished (6), we neglected CYP3A5 in our clarithromycin and midazolam models, since it was reported that CYP3A5 plays a negligible role in the PK of both CYP3A substrates (32,98,99).

The PK of clarithromycin further depends on the distribution into MN and PMN *in vivo*. Since the standard

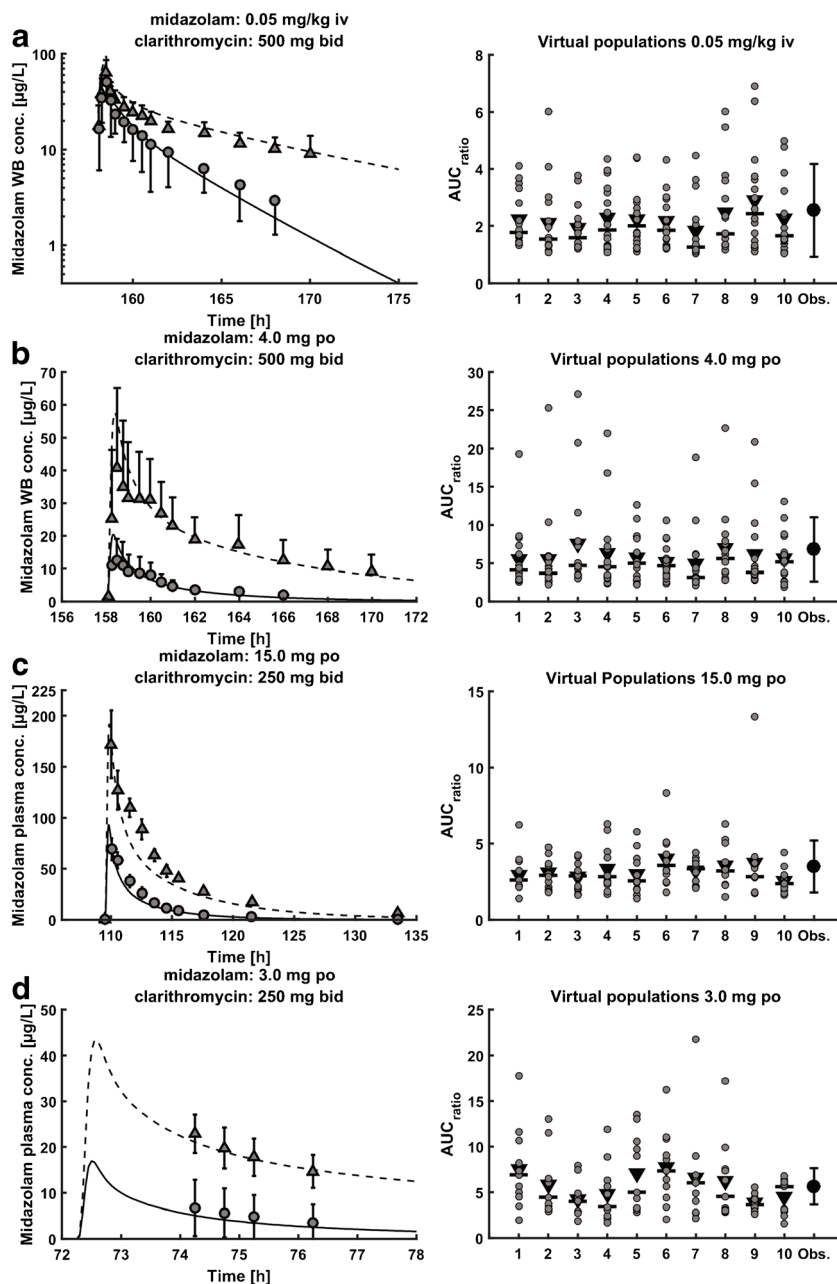


Fig. 5. *Left column:* predicted concentration-time profiles of intravenous and oral doses of midazolam (**a, b**: ref. (29), **c**: ref. (39), **d**: ref. (36)) with and without prior clarithromycin regimens in comparison with observed mean data (\pm standard deviation (SD)). *Solid line*, predicted midazolam mean without prior clarithromycin; *dashed line*, predicted midazolam mean with prior clarithromycin; *gray circles*, observed mean midazolam without prior clarithromycin; *gray triangles*, observed mean midazolam with prior clarithromycin. *Right column:* predicted midazolam AUC_{ratio} ($AUC_{inhibition}/AUC_{normal}$) in 10 virtual populations of intravenous and oral doses of midazolam in comparison with observed mean data (\pm SD). *Horizontal lines*, predicted midazolam AUC_{ratio} median; *triangles*, predicted midazolam AUC_{ratio} mean; *gray circles*, predicted individual midazolam AUC_{ratio} s; *filled circles*, observed mean midazolam AUC_{ratio} (\pm SD). Clarithromycin was administered orally (bid) with 250 mg (36,39) and 500 mg (29). *WB* whole blood

whole-body PK-Sim model does not offer MN or PMN cell compartments, we used the RBC compartments (with adjusted permeability values) as surrogate compartments for RBC + (MN + PMN) cells to adequately describe the PK of clarithromycin. In a clinical study with 250 mg bid dosing, the

observed peak concentrations (C_{max}) of clarithromycin in MN and PMN cells were 29 and 17 $\mu\text{g}/\text{mL}$, respectively, leading to a C_{max} concentration ratio $C_{max,MN+PMN}/C_{max,plasma}$ of 10 to 30 in healthy volunteers (27). The observed C_{max} values correspond to an amount of 17 mg of clarithromycin. The

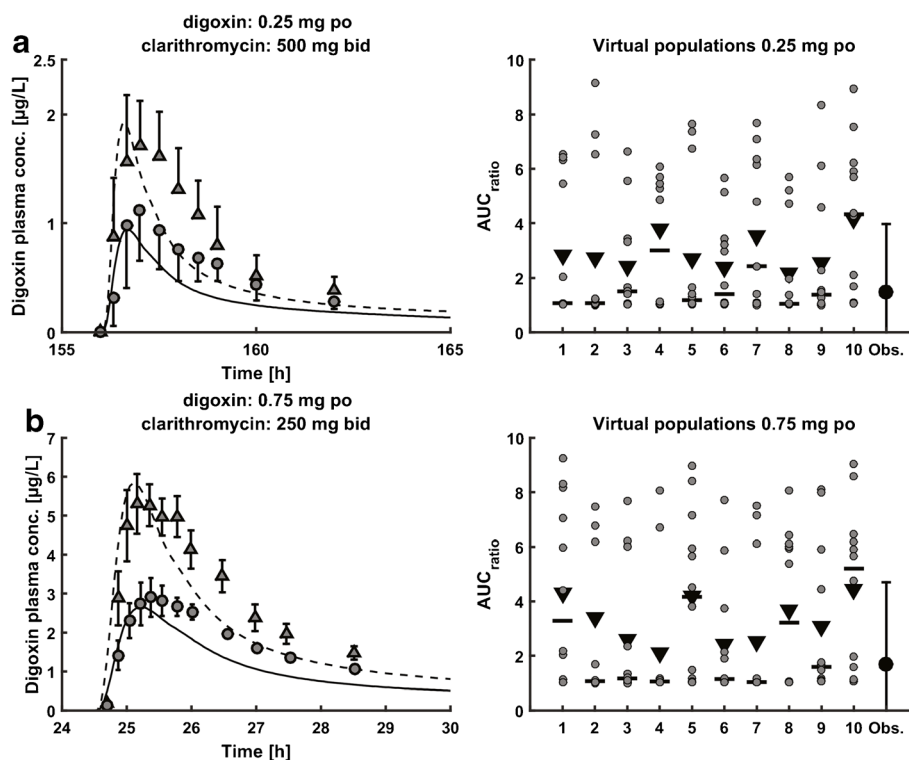


Fig. 6. Left column: predicted concentration-time profiles of digoxin after single oral doses of digoxin (a: ref. (48), b: ref. (26)) with and without prior clarithromycin regimens in comparison with observed mean data (\pm standard deviation (SD)). Solid line, predicted digoxin mean without prior clarithromycin; dashed line, predicted digoxin mean with prior clarithromycin; gray circles, observed mean digoxin without prior clarithromycin; gray triangles, observed mean digoxin with prior clarithromycin. Right column: predicted digoxin AUC_{ratio} ($AUC_{inhibition}/AUC_{normal}$) in 10 virtual populations of oral digoxin in comparison with observed mean data (\pm SD). Horizontal lines, predicted digoxin AUC_{ratio} median; triangles, predicted digoxin AUC_{ratio} mean; gray circles, predicted individual digoxin AUC_{ratios} ; filled circles, observed mean digoxin AUC_{ratio} (\pm SD). Clarithromycin was administered orally (bid) with 250 mg (26) and 500 mg (48)

predicted, additional amount of clarithromycin in the RBC compartments, due to the optimized asymmetrical permeability ratio of 13, was 36 mg, which is reasonably close.

In the final digoxin model, digoxin is binding to the ATP1A2 ATPase. The ATPase concentration was fitted to a reference concentration in the brain of 99.5 μ mol/L. ATPase

measurements of [3H]-ouabain binding, enzyme activity and maximum transport capacity suggest that the concentration of Na^+K^+ pumps (ATPase) in mammalian skeletal muscle is about 300–800 pmol/g wet tissue (100), which translates to 0.4–1.1 μ mol/L, assuming a tissue density of 1 g/mL and an expression level of 0.7 in muscle. The reason for this discrepancy

Table III. Comparison Predicted vs. Observed AUC Ratio

Application and dose [mg] of clarithromycin	Application and dose [mg] of victim drug	Number	Females [%]	Predicted mean $AUC_{ratio}^a \pm$ STD	Observed mean $AUC_{ratio} \pm$ STD	$AUC_{ratio,predicted}/AUC_{ratio,observed}$	Ref.
Midazolam							
po (tab, MD), 500	iv (inf, 30 min), 0.05/kg	16	50	2.2 \pm 1.2	2.8 \pm 1.6	0.8	(29)
po (tab, MD), 250	po (sol, SD), 3.0	11	10	5.8 \pm 3.7	5.6 \pm 2.0	1.0	(36) ^b
po (tab, MD), 500	po (tab, SD), 4.0	16	50	5.9 \pm 4.6	7.0 \pm 4.2	0.8	(29)
po (tab, MD), 250	po (tab, SD), 15.0	12	66	3.2 \pm 1.5	3.6 \pm 1.7	0.9	(39)
Digoxin							
po (tab, MD), 400	iv (inf, 60 min), 0.5	9	0	1.01 \pm 0.01	0.98 \pm 2.22	1.0	(45)
po (tab, MD), 250	iv (inf, 4 min), 0.01/kg	12	0	1.02	1.2	0.9	(26)
po (tab, MD), 500	po (tab, SD), 0.25	18	50	2.91 \pm 2.74	1.47 \pm 2.50	2.0	(48)
po (tab, MD), 250	po (tab, SD), 0.75	12	0	3.37 \pm 2.86	1.7 \pm 3.05	2.0	(26)

inf infusion, iv intravenous, MD multiple doses, po per os, SD single dose, sol solution, STD standard deviation, tab tablet

^a $AUC_{ratio} = AUC_{inhibition}/AUC_{normal}$

^b Individual concentration-time profiles are unpublished in-house data

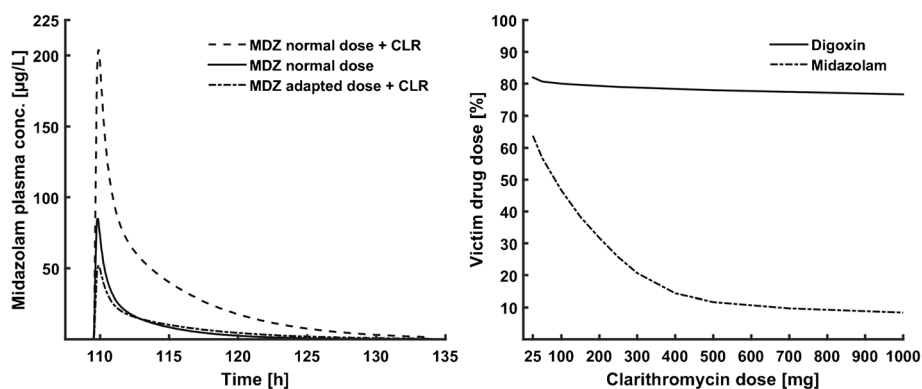


Fig. 7. Left: predicted concentration-time profiles of midazolam after single oral doses of midazolam (MDZ) with and without oral clarithromycin (CLR) pretreatment. *Solid line*, 100% midazolam dose without clarithromycin; *dashed line*, 100% midazolam dose with clarithromycin; *dashed-dotted line*, adapted 26% midazolam dose with clarithromycin. Right: victim drug dose recommendations in percent depending on the co-administered clarithromycin dose at clarithromycin steady state (bid). *Solid line*, adapted digoxin dose; *dashed-dotted line*, adapted midazolam dose

is unknown and probably reflects further mechanisms of digoxin distribution that we have not understood so far.

The performance of the clarithromycin–midazolam model is very good over the full range of administered doses and administration protocols including the predicted mean AUC_{ratio} and corresponding standard deviations. Consequently, this model can help to replace ketoconazole by guiding clinical DDI study designs with clarithromycin as a strong mechanism-based inhibitor of CYP3A4. Although a secondary objective, the clarithromycin–digoxin model shows very good performance. Nevertheless, the predicted mean AUC_{ratio} of oral digoxin (0.25, 0.75 mg) with and without clarithromycin pretreatment is over-predicted by a factor of 2. Interestingly, the predicted median AUC_{ratio} is close to the observed mean. Virtual population simulations revealed a wide range of individual AUC_{ratio} s between 1 and 10 (Fig. 6). There is no over-prediction using a single mean study individual, instead of a population, to predict the AUC_{ratio} for, e.g., 0.25 mg digoxin (predicted, 1.33; observed, 1.47). The reason for the over-prediction lies in the combination of intestinal permeability of digoxin together with the mucosal P-gp activities along the intestinal tract within the virtual populations. This combination leads to a high sensitivity to P-gp transport for some individuals which in turn leads to the skewed distribution of concentration-time profiles (predicted median AUC_{ratio} < predicted mean AUC_{ratio}). Further, knowledge on tissue-specific P-gp expression and its variability would greatly improve the DDI population predictions. This may also include genetic information because P-gp polymorphisms have been related to differences in digoxin distribution (101) and also to important clinical endpoints in digoxin users (102). It could also be speculated that unbound tissue concentrations of clarithromycin and/or digoxin are not adequately predicted.

Our dose adaptation analysis identified that the recommended digoxin dose is constant at ~80% across the investigated dose range, whereas the dose of midazolam is declining from 60 to 10% for clarithromycin doses of 25 to 500 mg bid, respectively. For higher clarithromycin doses (>500 mg), no further reduction of the midazolam dose seems to be required. For oral digoxin, the

competitive DDI with clarithromycin occurs predominantly in the mucosa where clarithromycin reaches local concentrations high enough to significantly inhibit the P-gp transport of digoxin even at clarithromycin doses of 25 mg. In contrast, 500 mg clarithromycin at steady state are necessary to reach the maximum MBI for CYP3A4. For clinical practice, this could imply that a single dose adaptation is sufficient for digoxin but a number of midazolam dose adaptations might be needed, depending on the given clarithromycin dose. There are several approved oral formulations and strengths available for midazolam and digoxin in the USA. According to the FDA “Orange Book,” midazolam is approved and available as an oral syrup (2 mg base/mL) and digoxin is available as oral solution (0.05 mg/mL) and tablet (0.125 and 0.25 mg). The accurate administration of the adapted doses of midazolam and digoxin is feasible with the oral solution formulations. Training in appropriate dosing of the oral solutions might be needed for the patients.

Since DDIs are a major reason for adverse events during commonplace pharmacotherapy, the FDA labels would benefit from dosing guidance to prevent avoidable DDIs with clarithromycin, midazolam, and digoxin. To assess the impact of dose adaptations on DDIs in a population, simulations could help to close this gap in the respective labels. The virtual population simulations with the adapted victim drug doses in supplementary Table 1 show that a dose adaptation is especially helpful and necessary during the MBI (clarithromycin–midazolam). Although the adapted doses prevent digoxin overdosing during the competitive inhibition (clarithromycin–digoxin) in a significant number of individuals, the reduction of individuals experiencing strong and moderate AUC changes is improvable. However, as a drug with a narrow therapeutic index, digoxin is a typical candidate drug for therapeutic drug monitoring which implies that the individualization of the digoxin dose during clarithromycin co-treatment in this study especially revolves around the determination of the digoxin starting dose. A clinical study should be considered to evaluate and add more confidence to these model predictions established in a virtual population.

Comprehensive and mechanistic whole-body PBPK models are complex and require the input of many parameters. For some of these parameters, no values are available from the literature or the reported values differ strongly. The parameter sensitivity analysis shows that the predicted DDI AUC_{ratios} are sensitive to 5 out of 10 assessed parameters. Among these 5 parameters, especially CYP3A4 liver half-life but also CYP3A4 K_I and CYP3A4 k_{inact} cannot be reliably derived from the literature. The liver half-life of CYP3A4 is reported with values from 10 to 140 h. We found that a half-life of 36 h was optimal to describe the effects of the MBI by clarithromycin. The same value has been reported as most appropriate in a dedicated modeling study by Rowland Yeo *et al.* using several CYP3A4 mechanism-dependent inhibitors and victim drugs (103). For CYP3A4 K_I and k_{inact} , the values used in the simulations were the only ones to result in an accurate description of the clinical clarithromycin data. Additional impactful parameters were the midazolam CYP3A4 k_{cat} and the digoxin P-gp k_{cat} . Both values have been optimized very carefully using a multitude of clinical studies spanning large dosing ranges of intravenous and oral application. In addition, the digoxin model has been developed including data on the fraction of digoxin excreted in urine, to increase our confidence in the optimized P-gp k_{cat} value. However, this sensitivity analysis demonstrates that the MBI of clarithromycin with CYP3A4 is strongly influenced by 3 different parameters (CYP3A4 liver half-life, CYP3A4 K_I , and CYP3A4 k_{inact}). We will continue to evaluate our DDI model by expanding it to the interactions with other victim drugs and the scientific community will probably carry on to investigate these parameters until a good validation is reached. On the *in vivo* side, these results suggest that interindividual differences in CYP3A4 and P-gp activity, CYP3A4 turnover in the liver and clarithromycin concentrations available to cause the MBI of CYP3A4 will lead to large interindividual differences in the observed AUC_{ratios} during this DDI. If this is true, DDI modeling should strive to account for these variabilities for accurate dose recommendations and study design.

In summary, our work shows that the sub-compartmentalization of blood into plasma and red blood cell compartments is not sufficient to account for important distribution processes found *in vivo* for clarithromycin. This might also hold true for other eligible compounds. As models will become more mechanistic in the future and the spatial and temporal resolution will be continuously improved, a more detailed compartmentalization of the blood will be part of a general trend for more accurate descriptions of organs important for absorption, disposition, action, and toxicity (gut, liver, kidney, brain, etc.).

Further direction for future work is the measurement and the interplay of many important parameters needed as inputs for model building which are not (publicly) available yet, starting with physicochemical parameters, activity levels of drug metabolizing enzymes and transporters throughout the body and other parameters to inform ADME and DDI processes. Also, the characterization of the interindividual variability of these parameters would greatly help to understand individual differences in observed plasma concentrations and could be considered during model building.

CONCLUSION

In this paper, we present the first published whole-body PBPK model of clarithromycin. Our clarithromycin model was linked to PBPK models of the paradigm victim drugs midazolam and digoxin and was capable to predict the resulting DDIs. With the presented model, we provide a valuable, publicly available tool for drug development and clinical practice. The presented models can help researchers understand and characterize the DDI potential of new molecular entities and inform the design of DDI studies with potential CYP3A4 and P-gp substrates.

REFERENCES

1. Pirmohamed M, James S, Meakin S, *et al.* Adverse drug reactions as cause of admission to hospital: prospective analysis of 18 820 patients. *BMJ*. 2004;329:15–9. doi:10.1136/bmj.329.7456.15.
2. Huang S-M, Lesko LJ. Drug-drug, drug-dietary supplement, and drug-citrus fruit and other food interactions: what have we learned? *J Clin Pharmacol*. 2004;44:559–69. doi:10.1177/0091270004265367.
3. EMA. Guideline on the investigation of drug interactions. 2012. http://www.ema.europa.eu/docs/en_GB/document_library/Scientific_guideline/2012/07/WC500129606.pdf. Accessed 28 Jan 2016.
4. FDA. Guidance for industry. Drug interaction studies study design, data analysis, implications for dosing, and labeling recommendations. 2012. <http://www.fda.gov/downloads/Drugs/GuidanceComplianceRegulatoryInformation/Guidances/UCM292362.pdf>. Accessed 28 Jan 2016.
5. Lin JH. CYP induction-mediated drug interactions: in vitro assessment and clinical implications. *Pharm Res*. 2006;23:1089–116. doi:10.1007/s11095-006-0277-7.
6. Wilkinson GR. Drug metabolism and variability among patients in drug response. *N Engl J Med*. 2005;352:2211–21. doi:10.1056/NEJMra032424.
7. Zhao P, Ragueneau-Majlessi I, Zhang L, *et al.* Quantitative evaluation of pharmacokinetic inhibition of CYP3A substrates by ketoconazole: a simulation study. *J Clin Pharmacol*. 2009;49:351–9. doi:10.1177/0091270008331196.
8. FDA. FDA advises against using oral ketoconazole in drug interaction studies due to serious potential side effects. 2013. <http://www.fda.gov/Drugs/DrugSafety/ucm371017.htm>. Accessed 28 Jan 2016.
9. Ke AB, Zamek-Gliszczyński MJ, Higgins JW, Hall SD. Itraconazole and clarithromycin as ketoconazole alternatives for clinical CYP3A inhibition studies. *Clin Pharmacol Ther*. 2014;95:473–6. doi:10.1038/clpt.2014.41.
10. Goossens H, Ferech M, Coenen S, Stephens P. Comparison of outpatient systemic antibacterial use in 2004 in the United States and 27 European countries. *Clin Infect Dis*. 2007;44:1091–5. doi:10.1086/512810.
11. Rodrigues AD, Roberts EM, Mulford DJ, Yao Y, Ouellet D. Oxidative metabolism of clarithromycin in the presence of human liver microsomes. Major role for the cytochrome P4503A (CYP3A) subfamily. *Drug Metab Dispos*. 1997;25:623–30.
12. Mayhew BS, Jones DR, Hall SD. An in vitro model for predicting in vivo inhibition of cytochrome P450 3A4 by metabolic intermediate complex formation. *Drug Metab Dispos*. 2000;28:1031–7.
13. Chu SY, Sennello LT, Bunnell ST, Varga LL, Wilson DS, Sonders RC. Pharmacokinetics of clarithromycin, a new macrolide, after single ascending oral doses. *Antimicrob Agents Chemother*. 1992;36:2447–53. doi:10.1128/AAC.36.11.2447.

14. Saito H, Fukasawa Y, Otsubo Y, Yamada K, Sezaki H, Yamashita S. Carrier-mediated transport of macrolide antimicrobial agents across Caco-2 cell monolayers. *Pharm Res*. 2000;17:761–5. doi:10.1023/A:1007550820196.
15. Eberl S, Renner B, Neubert A, *et al.* Role of p-glycoprotein inhibition for drug interactions: evidence from in vitro and pharmacoepidemiological studies. *Clin Pharmacokinet*. 2007;46:1039–49. doi:10.2165/00003088-200746120-00004.
16. Yabe Y, Galetin A, Houston JB. Kinetic characterization of rat hepatic uptake of 16 actively transported drugs. *Drug Metab Dispos*. 2011;39:1808–14. doi:10.1124/dmd.111.040477.
17. Garver E, Hugger ED, Shearn SP, *et al.* Involvement of intestinal uptake transporters in the absorption of azithromycin and clarithromycin in the rat. *Drug Metab Dispos*. 2008;36:2492–8. doi:10.1124/dmd.108.022285.
18. Seithel A, Eberl S, Singer K, *et al.* The influence of macrolide antibiotics on the uptake of organic anions and drugs mediated by OATP1B1 and OATP1B3. *Drug Metab Dispos*. 2007;35:779–86. doi:10.1124/dmd.106.014407.
19. Patki KC, Von Moltke LL, Greenblatt DJ. In vitro metabolism of midazolam, triazolam, nifedipine, and testosterone by human liver microsomes and recombinant cytochromes p450: role of cyp3a4 and cyp3a5. *Drug Metab Dispos*. 2003;31:938–44. doi:10.1124/dmd.31.7.938.
20. Koup JR, Greenblatt DJ, Jusko WJ, Smith TW, Koch-Weser J. Pharmacokinetics of digoxin in normal subjects after intravenous bolus and infusion doses. *J Pharmacokinet Biopharm*. 1975;3:181–92. doi:10.1007/BF00162306.
21. Ito S, Woodland C, Harper PA, Koren G. P-glycoprotein-mediated renal tubular secretion of digoxin: the toxicological significance of the urine-blood barrier model. *Life Sci*. 1993;53:PL25–31. doi:10.1016/0024-3205(93)90667-R.
22. Dostanic-Larson I. Physiological role of the 1- and 2-isoforms of the Na⁺-K⁺-ATPase and biological significance of their cardiac glycoside binding site. *AJP Regul Integr Comp Physiol*. 2005;290:R524–8. doi:10.1152/ajpregu.00838.2005.
23. Lappin G, Shishikura Y, Jochemsen R, *et al.* Comparative pharmacokinetics between a microdose and therapeutic dose for clarithromycin, sumatriptan, propafenone, paracetamol (acetaminophen), and phenobarbital in human volunteers. *Eur J Pharm Sci*. 2011;43:141–50. doi:10.1016/j.ejps.2011.04.009.
24. Chu SY, Deaton R, Cavanaugh J. Absolute bioavailability of clarithromycin after oral administration in humans. *Antimicrob Agents Chemother*. 1992;36:1147–50. doi:10.1128/AAC.36.5.1147.
25. Chu S, Wilson DS, Deaton RL, Mackenthun AV, Eason CN, Cavanaugh JH. Single- and multiple-dose pharmacokinetics of clarithromycin, a new macrolide antimicrobial. *J Clin Pharmacol*. 1993;33:719–26. doi:10.1002/j.1552-4604.1993.tb05613.x.
26. Rengelshausen J, Göggelmann C, Burhenne J, *et al.* Contribution of increased oral bioavailability and reduced nonglomerular renal clearance of digoxin to the digoxin-clarithromycin interaction. *Br J Clin Pharmacol*. 2003;56:32–8. doi:10.1046/j.1365-2125.2003.01824.x.
27. Kees F, Wellenhofer M, Grobecker H. Serum and cellular pharmacokinetics of clarithromycin 500 mg q.d. and 250 mg b.i.d. in volunteers. *Infection*. 1995;23:168–72. doi:10.1007/BF01793859.
28. Abduljalil K, Kinzig M, Bulitta J, *et al.* Modeling the autoinhibition of clarithromycin metabolism during repeated oral administration. *Antimicrob Agents Chemother*. 2009;53:2892–901. doi:10.1128/AAC.01193-08.
29. Gorski JC, Jones DR, Haehner-Daniels BD, Hamman MA, O'Mara EM, Hall SD. The contribution of intestinal and hepatic CYP3A to the interaction between midazolam and clarithromycin. *Clin Pharmacol Ther*. 1998;64:133–43. doi:10.1016/S0009-9236(98)90146-1.
30. Brown CR, Sarnquist FH, Canup CA, Pedley TA. Clinical, electroencephalographic, and pharmacokinetic studies of a water-soluble benzodiazepine, midazolam maleate. *Anesthesiology*. 1979;50:467–70.
31. van Rongen A, Kervezee L, Brill M, *et al.* Population pharmacokinetic model characterizing 24-hour variation in the pharmacokinetics of oral and intravenous midazolam in healthy volunteers. *CPT pharmacometrics. Syst Pharmacol*. 2015;4:454–64. doi:10.1002/psp4.12007.
32. Yu K. Effect of the CYP3A5 genotype on the pharmacokinetics of intravenous midazolam during inhibited and induced metabolic states. *Clin Pharmacol Ther*. 2004;76:104–12. doi:10.1016/j.clpt.2004.03.009.
33. Smith MT, Eadie MJ, Brophy TO. The pharmacokinetics of midazolam in man. *Eur J Clin Pharmacol*. 1981;19:271–8. doi:10.1007/BF00562804.
34. Hardmeier M, Zimmermann R, Rüegg S, *et al.* Intranasal midazolam: pharmacokinetics and pharmacodynamics assessed by quantitative EEG in healthy volunteers. *Clin Pharmacol Ther*. 2012;91:856–62. doi:10.1038/clpt.2011.316.
35. Heizmann P, Eckert M, Ziegler WH. Pharmacokinetics and bioavailability of midazolam in man. *Br J Clin Pharmacol*. 1983;16 Suppl 1:43S–9. doi:10.1111/j.1365-2125.1983.tb02270.x.
36. Markert C, Hellwig R, Burhenne J, *et al.* Interaction of ambrisentan with clarithromycin and its modulation by polymorphic SLCO1B1. *Eur J Clin Pharmacol*. 2013;69:1785–93. doi:10.1007/s00228-013-1529-1.
37. Zhou D, Lu Z, Sunzel M, Xu H, Al-Huniti N. Population pharmacokinetic modelling to assess clinical drug-drug interaction between AZD7325 and midazolam. *J Clin Pharm Ther*. 2014;39:404–10. doi:10.1111/jcpt.12152.
38. Bornemann LD, Min BH, Crews T, *et al.* Dose dependent pharmacokinetics of midazolam. *Eur J Clin Pharmacol*. 1985;29:91–5. doi:10.1007/BF00547375.
39. Yeates RA, Laufen H, Zimmermann T. Interaction between midazolam and clarithromycin: comparison with azithromycin. *Int J Clin Pharmacol Ther*. 1996;34:400–5.
40. Kramer WG, Kolibash AJ, Lewis RP, Bathala MS, Visconti J, Reaming RH. Pharmacokinetics of digoxin: relationship between response intensity and predicted compartmental drug levels in man. *J Pharmacokinet Biopharm*. 1979;7:47–61. doi:10.1007/BF01059440.
41. Wagner JG, Popat KD, Das SK, Sakmar E, Movahhed H. Evidence of nonlinearity in digoxin pharmacokinetics. *J Pharmacokinet Biopharm*. 1981;9:147–66. doi:10.1007/BF01068079.
42. Steiness E, Waldorff S, Hansen PB. Renal digoxin clearance: dependence on plasma digoxin and diuresis. *Eur J Clin Pharmacol*. 1982;23:151–4. doi:10.1007/BF00545970.
43. Ding R, Tayrouz Y, Riedel K, *et al.* Substantial pharmacokinetic interaction between digoxin and ritonavir in healthy volunteers. *Clin Pharmacol Ther*. 2004;76:73–84. doi:10.1016/j.clpt.2004.02.008.
44. Greiner B, Eichelbaum M, Fritz P, *et al.* The role of intestinal P-glycoprotein in the interaction of digoxin and rifampin. *J Clin Invest*. 1999;104:147–53. doi:10.1172/JCI16663.
45. Tsutsumi K, Kotegawa T, Kuranari M, *et al.* The effect of erythromycin and clarithromycin on the pharmacokinetics of intravenous digoxin in healthy volunteers. *J Clin Pharmacol*. 2002;42:1159–64. doi:10.1177/009127002237992.
46. Ochs HR, Greenblatt DJ, Bodem G, Harmatz JS. Dose-independent pharmacokinetics of digoxin in humans. *Am Heart J*. 1978;96:507–11. doi:10.1016/0002-8703(78)90162-X.
47. Becquemont L, Verstuyft C, Kerb R, *et al.* Effect of grapefruit juice on digoxin pharmacokinetics in humans. *Clin Pharmacol Ther*. 2001;70:311–6. doi:10.1067/mcp.2001.118867.
48. Gurley BJ, Swain A, Williams DK, Barone G, Battu SK. Gauging the clinical significance of P-glycoprotein-mediated herb-drug interactions: comparative effects of St. John's wort, Echinacea, clarithromycin, and rifampin on digoxin pharmacokinetics. *Mol Nutr Food Res*. 2008;52:772–9. doi:10.1002/mnfr.200700081.
49. Eckermann G, Lahu G, Nassr N, Bethke TD. Absence of pharmacokinetic interaction between roflumilast and digoxin in healthy adults. *J Clin Pharmacol*. 2012;52:251–7. doi:10.1177/0091270010389467.
50. Oosterhuis B, Jonkman JH, Andersson T, Zuiderwijk PB, Jedema JN. Minor effect of multiple dose omeprazole on the pharmacokinetics of digoxin after a single oral dose. *Br J Clin Pharmacol*. 1991;32:569–72. doi:10.1111/j.1365-2125.1991.tb03953.x.

51. Kirch W, Logemann C, Heidemann H, Santos SR, Ohnhaus EE. Effect of two different doses of nitrendipine on steady-state plasma digoxin level and systolic time intervals. *Eur J Clin Pharmacol*. 1986;31:391–5. doi:10.1007/BF00613512.
52. Qiu R, Plowchalk DR, Byon W, Terra SG, Corrigan B, Mordenti J, *et al.* Lack of a pharmacokinetic interaction between dimebon (latrepirdine) and digoxin in healthy subjects. ASCPT 2010 Annual Meeting, Atlanta, Georgia, USA, 17th–20th March. *Clin Pharmacol Ther*. 2010;87(S1):S91:PIII–72. doi:10.1038/clpt.2009.277.
53. Friedrich C, Ring A, Brand T, Sennewald R, Graefe-Mody EU, Woerle HJ. Evaluation of the pharmacokinetic interaction after multiple oral doses of linagliptin and digoxin in healthy volunteers. *Eur J Drug Metab Pharmacokinet*. 2011;36:17–24. doi:10.1007/s13318-011-0028-y.
54. Vaidyanathan S, Camenisch G, Schuetz H, *et al.* Pharmacokinetics of the oral direct renin inhibitor aliskiren in combination with digoxin, atorvastatin, and ketoconazole in healthy subjects: the role of P-glycoprotein in the disposition of aliskiren. *J Clin Pharmacol*. 2008;48:1323–38. doi:10.1177/0091270008323258.
55. Nožinić D, Milić A, Mikac L, Ralić J. Assessment of macrolide transport using PAMPA, Caco-2 and MDCKII-hMDR1 assays. *Croat Chem Acta*. 2010;83:323–31.
56. Wheeler DL, Church DM, Federhen S, *et al.* Database resources of the national center for biotechnology. *Nucleic Acids Res*. 2003;31:28–33. doi:10.1093/nar/gks1189.
57. Meyer M, Schneckener S, Ludewig B, Kuepfer L, Lippert J. Using expression data for quantification of active processes in physiologically based pharmacokinetic modeling. *Drug Metab Dispos*. 2012;40:892–901. doi:10.1124/dmd.111.043174.
58. Ge X, Yamamoto S, Tsutsumi S, *et al.* Interpreting expression profiles of cancers by genome-wide survey of breadth of expression in normal tissues. *Genomics*. 2005;86:127–41. doi:10.1016/j.ygeno.2005.04.008.
59. Rodrigues AD. Integrated cytochrome P450 reaction phenotyping: attempting to bridge the gap between cDNA-expressed cytochromes P450 and native human liver microsomes. *Biochem Pharmacol*. 1999;57:465–80. doi:10.1016/S0006-2952(98)00268-8.
60. Badée J, Achour B, Rostami-Hodjegan A, Galetin A. Meta-analysis of expression of hepatic organic anion-transporting polypeptide (OATP) transporters in cellular systems relative to human liver tissue. *Drug Metab Dispos*. 2015;43:424–32. doi:10.1124/dmd.114.062034.
61. Nishimura M, Naito S. Tissue-specific mRNA expression profiles of human ATP-binding cassette and solute carrier transporter superfamilies. *Drug Metab Pharmacokinet*. 2005;20:452–77. doi:10.2133/dmpk.20.452.
62. Tucker TGHA, Milne AM, Fournel-Gigleux S, Fenner KS, Coughtrie MWH. Absolute immunoquantification of the expression of ABC transporters P-glycoprotein, breast cancer resistance protein and multidrug resistance-associated protein 2 in human liver and duodenum. *Biochem Pharmacol*. 2012;83:279–85. doi:10.1016/j.bcp.2011.10.017.
63. Rodvold KA. Clinical pharmacokinetics of clarithromycin. *Clin Pharmacokinet*. 1999;37:385–98. doi:10.2165/00003088-199937050-00003.
64. Obach RS, Lombardo F, Waters NJ. Trend analysis of a database of intravenous pharmacokinetic. *Pharmacology*. 2008;36:1385–405. doi:10.1124/dmd.108.020479.
65. Quinney SK, Haehner BD, Rhoades MB, Lin Z, Gorski JC, Hall SD. Interaction between midazolam and clarithromycin in the elderly. *Br J Clin Pharmacol*. 2008;65:98–109. doi:10.1111/j.1365-2125.2007.02970.x.
66. Allonen H, Ziegler G, Klotz U. Midazolam kinetics. *Clin Pharmacol Ther*. 1981;30:653–61. doi:10.1038/clpt.1981.217.
67. Doucet-Populaire F, Capobianco JO, Zakula D, Jarlier V, Goldman RC. Molecular basis of clarithromycin activity against *Mycobacterium avium* and *Mycobacterium smegmatis*. *J Antimicrob Chemother*. 1998;41:179–87. doi:10.1093/jac/41.2.179.
68. Atkinson HC, Begg EJ. Relationship between human milk lipid-ultrafiltrate and octanol-water partition coefficients. *J Pharm Sci*. 1988;77:796–8. doi:10.1002/jps.2600770916.
69. Mulla H, McCormack P, Lawson G, Firmin RK, Upton DR. Pharmacokinetics of midazolam in neonates undergoing extracorporeal membrane oxygenation. *Anesthesiology*. 2003;99(2):275–82.
70. Arellano C, Philibert C, Vachoux C, Woodley J, Houin G. The metabolism of midazolam and comparison with other CYP enzyme substrates during intestinal absorption: in vitro studies with rat everted gut sacs. *J Pharm Pharm Sci Publ Can Soc Pharm Sci Soc Can Sci Pharm*. 2007;10:26–36.
71. Yamano K, Yamamoto K, Katashima M, *et al.* Prediction of midazolam-CYP3A inhibitors interaction in the human liver from in vivo/in vitro absorption, distribution, and metabolism data. *Drug Metab Dispos*. 2001;29:443–52.
72. Zhang X-R, Chen X-Y, Hu L-D, Tang X, Li S-M, Zhong D-F. Evaluation of in-vitro dissolution and in-vivo absorption for two different film-coated pellets of clarithromycin. *Arch Pharm Res*. 2005;28:977–82. doi:10.1007/BF02973886.
73. McFarland JW, Berger CM, Froshauer S, *et al.* Quantitative structure-activity relationships among macrolide antibacterial agents: in vitro and in vivo potency against *Pasteurella multocida*. *J Med Chem*. 1997;40:1340–6. doi:10.1021/jm960436i.
74. Liu Y, Hunt CA. Studies of intestinal drug transport using an in silico epithelio-mimetic device. *BioSystems*. 2005;82:154–67. doi:10.1016/j.biosystems.2005.06.008.
75. Walser A, Benjamin LE, Flynn T, Mason C, Schwartz R, Fryer RI. Quinazolines and 1,4-benzodiazepines. 84. Synthesis and reactions of imidazo[1,5-a][1,4]benzodiazepines. *J Org Chem*. 1978;43:936–44. doi:10.1021/jo00399a029.
76. Salem II, Düzgünes N. Efficacies of cyclodextrin-complexed and liposome-encapsulated clarithromycin against *Mycobacterium avium* complex infection in human macrophages. *Int J Pharm*. 2003;250:403–14. doi:10.1016/S0378-5173(02)00552-5.
77. Alsenz J, Meister E, Haenel E. Development of a partially automated solubility screening (PASS) assay for early drug development. *J Pharm Sci*. 2007;96:1748–62. doi:10.1002/jps.20814.
78. Loftsson T, Hreinsdóttir D. Determination of aqueous solubility by heating and equilibration: a technical note. *AAPS PharmSciTech*. 2006;7, E4. doi:10.1208/pt070104.
79. Rautio J, Humphreys JE, Webster LO, *et al.* In vitro P-glycoprotein inhibition assays for assessment of clinical drug interaction potential of new drug candidates: a recommendation for probe substrates. *Drug Metab Dispos*. 2006;34:786–92. doi:10.1124/dmd.105.008615.paper.
80. Gertz M, Harrison A, Houston JB, Galetin A. Prediction of human intestinal first-pass metabolism of 25 CYP3A substrates from in vitro clearance and permeability data. *Drug Metab Dispos*. 2010;38:1147–58. doi:10.1124/dmd.110.032649.
81. Galetin A, Brown C, Hallifax D, Ito K, Houston JB. Utility of recombinant enzyme kinetics in prediction of human clearance: impact of variability, CYP3A5, and CYP2C19 on CYP3A4 probe substrates. *Drug Metab Dispos*. 2004;32:1411–20. doi:10.1124/dmd.104.000844.
82. Stephens RH, O'Neill CA, Warhurst A, Carlson GL, Rowland M, Warhurst G. Kinetic profiling of P-glycoprotein-mediated drug efflux in rat and human intestinal epithelia. *J Pharmacol Exp Ther*. 2001;296:584–91.
83. Katz A, Lifshitz Y, Bab-Dinitz E, *et al.* Selectivity of digitalis glycosides for isoforms of human Na,K-ATPase. *J Biol Chem*. 2010;285:19582–92. doi:10.1074/jbc.M110.119248.
84. Polasek TM, Miners JO. Quantitative prediction of macrolide drug-drug interaction potential from in vitro studies using testosterone as the human cytochrome P4503A substrate. *Eur J Clin Pharmacol*. 2006;62:203–8. doi:10.1007/s00228-005-0091-x.
85. Ito K, Ogihara K, Kanamitsu S, Itoh T. Prediction of the in vivo interaction between midazolam and macrolides based on in vitro studies using human liver microsomes. *Drug Metab Dispos*. 2003;31:945–54. doi:10.1124/dmd.31.7.945.
86. Jones DR, Ekins S, Li L, Hall SD. Computational approaches that predict metabolic intermediate complex formation with CYP3A4 (+b5). *Drug Metab Dispos*. 2007;35(9):1466–75.
87. Sohlenius-Sternbeck A-K. Determination of the hepatocellularity number for human, dog, rabbit, rat and mouse livers from protein

- concentration measurements. *Toxicol Vit.* 2006;20:1582–6. doi:10.1016/j.tiv.2006.06.003.
88. Cheng Y, Prusoff WH. Relationship between the inhibition constant (K₁) and the concentration of inhibitor which causes 50 per cent inhibition (I₅₀) of an enzymatic reaction. *Biochem Pharmacol.* 1973;22:3099–108.
 89. Shimada T, Yamazaki H, Mimura M, Inui Y, Guengerich FP. Interindividual variations in human liver cytochrome P-450 enzymes involved in the oxidation of drugs, carcinogens and toxic chemicals: studies with liver microsomes of 30 Japanese and 30 Caucasians. *J Pharmacol Exp Ther.* 1994;270:414–23.
 90. Venkatakrisnan K, Obach RS, Rostami-Hodjegan A. Mechanism-based inactivation of human cytochrome P450 enzymes: strategies for diagnosis and drug–drug interaction risk assessment. *Xenobiotica.* 2007;37:1225–56. doi:10.1080/00498250701670945.
 91. Yang J, Liao M, Shou M, *et al.* Cytochrome p450 turnover: regulation of synthesis and degradation, methods for determining rates, and implications for the prediction of drug interactions. *Curr Drug Metab.* 2008;9:384–94. doi:10.2174/138920008784746382.
 92. Prasad B, Evers R, Gupta A, *et al.* Interindividual variability in hepatic organic anion-transporting polypeptides and P-glycoprotein (ABCB1) protein expression: quantification by liquid chromatography tandem mass spectroscopy and influence of genotype, age, and sex. *Drug Metab Dispos.* 2013;42:78–88. doi:10.1124/dmd.113.053819.
 93. Rodgers T, Leahy D, Rowland M. Physiologically based pharmacokinetic modeling 1: predicting the tissue distribution of moderate-to-strong bases. *J Pharm Sci.* 2005;94:1259–76. doi:10.1002/jps.20322.
 94. Rodgers T, Rowland M. Physiologically based pharmacokinetic modelling 2: predicting the tissue distribution of acids, very weak bases, neutrals and zwitterions. *J Pharm Sci.* 2006;95:1238–57. doi:10.1002/jps.20502.
 95. Ishiguro M, Koga H, Kohno S, Hayashi T, Yamaguchi K, Hirota M. Penetration of macrolides into human polymorphonuclear leucocytes. *J Antimicrob Chemother.* 1989;24:719–29. doi:10.1093/jac/24.5.719.
 96. Quinney SK, Malireddy SR, Vuppalanchi R, *et al.* Rate of onset of inhibition of gut-wall and hepatic CYP3A by clarithromycin. *Eur J Clin Pharmacol.* 2013;69:439–48. doi:10.1007/s00228-012-1339-x.
 97. Quinney SK, Zhang X, Luckisiri A, Gorski JC, Li L, Hall SD. Physiologically based pharmacokinetic model of mechanism-based inhibition of CYP3A by clarithromycin. *Drug Metab Dispos.* 2010;38(2):241–8.
 98. Kharasch ED, Walker A, Isoherranen N, *et al.* Influence of CYP3A5 genotype on the pharmacokinetics and pharmacodynamics of the cytochrome P450A probes alfentanil and midazolam. *Clin Pharmacol Ther.* 2007;82:410–26. doi:10.1038/sj.cpt.6100237.
 99. Williams JA, Ring BJ, Cantrell VE, *et al.* Comparative metabolic capabilities of CYP3A4, CYP3A5, and CYP3A7. *Drug Metab Dispos.* 2002;30:883–91. doi:10.1124/dmd.30.8.883.
 100. Hansen O, Clausen T. Quantitative determination of Na⁺-K⁺-ATPase and other sarcolemmal components in muscle cells. *Am J Physiol.* 1988;254:C1–7.
 101. Comets E, Verstuyft C, Lavielle M, Jaillon P, Becquemont L, Mentré F. Modelling the influence of MDR1 polymorphism on digoxin pharmacokinetic parameters. *Eur J Clin Pharmacol.* 2007;63:437–49. doi:10.1007/s00228-007-0269-5.
 102. Niemeijer MN, van den Berg ME, Deckers JW, *et al.* ABCB1 gene variants, digoxin and risk of sudden cardiac death in a general population. *Heart.* 2015;101:1973–9. doi:10.1136/heartjnl-2014-307419.
 103. Rowland Yeo K, Walsky RL, Jamei M, Rostami-Hodjegan A, Tucker GT. Prediction of time-dependent CYP3A4 drug–drug interactions by physiologically based pharmacokinetic modelling: impact of inactivation parameters and enzyme turnover. *Eur J Pharm Sci.* 2011;43:160–73. doi:10.1016/j.ejps.2011.04.008.